Eur. Phys. J. C 47, 745–755 (2006)
Digital Object Identifier (DOI) 10.1140/epjc/s2006-02601-0

THE EUROPEAN PHYSICAL JOURNAL C

Masses and electroweak properties of light mesons in the relativistic quark model

D. Ebert[1], R.N. Faustov[1,2], V.O. Galkin[1,2,a]

[1] Institut für Physik, Humboldt–Universität zu Berlin, Newtonstr. 15, 12489 Berlin, Germany
[2] Dorodnicyn Computing Centre, Russian Academy of Sciences, Vavilov Str. 40, 119991 Moscow, Russia

Received: 3 November 2005 / Revised version: 5 May 2006 /
Published online: 30 June 2006 –

Abstract. The masses, pseudoscalar and vector weak decay constants and electromagnetic form factors of light S-wave mesons are studied in the framework of the relativistic quark model based on the quasipotential approach. We use the same model assumptions and parameters as in our previous investigations of heavy meson and baryon properties. The masses and wave functions of the ground state and radially excited π, ρ, K, K^* and ϕ mesons, obtained by solving numerically the relativistic Schrödinger-like equation with the complete relativistic $q\bar{q}$ potential including both spin-independent and spin-dependent terms, are presented. Novel relativistic expressions for the weak decay constants of the pseudoscalar and vector mesons are derived. It is shown that the intermediate negative-energy quark states give significant contributions which essentially decrease the decay constants bringing them in agreement with experimental data. The electromagnetic form factors of the pion, charged and neutral kaon are calculated in a broad range of the space-like momentum transfer. The corresponding charge radii are determined. All results agree well with the available experimental data.

PACS. 14.40.Aq; 13.40.Gp; 12.39.Ki

1 Introduction

The theoretical investigation of the properties of light mesons such as π, ρ, K, K^* and ϕ is a longstanding problem which plays an important role in understanding the low-energy QCD. The description of these mesons within the constituent quark model presents additional difficulties compared to heavy–light mesons and heavy quarkonia. In fact, due to the highly relativistic dynamics of light quarks, the v/c and $1/m_q$ expansions are completely inapplicable in the case of light mesons and the QCD coupling constant α_s at the related scale μ is rather large. Moreover, the behavior of $\alpha_s(\mu^2)$ in the infrared region is unknown and thus model dependent (exhibiting, e.g., freezing behavior, etc.). The pseudoscalar mesons π and K produce a special problem, since their small masses originate from their Goldstone nature caused by the broken chiral symmetry. Therefore the reliable description of light mesons requires the completely relativistic approach. It is well known that in the relativistic studies an important role is played by the Lorentz properties of the confining quark–antiquark interaction. The comparison of theoretical predictions with experimental data can provide valuable information on the form of the confining potential. Such information is of great practical interest, because at present it is not possible to obtain the relativistic $q\bar{q}$ potential in the whole range of distances from the basic principles of QCD.[1] Most of the main characteristics of light mesons are formed in the infrared (nonperturbative) region, thus providing important insight in the low-energy properties of $q\bar{q}$ interaction. Thus investigation of both static (e.g., masses and decay constants) and dynamic (e.g., electroweak decay form factors) properties is of significance.

Many different theoretical approaches have been used for studying light mesons, which are based on the relativized quark model [2], the Dyson–Schwinger and Bethe–Salpeter equations [3, 4], chiral quark models with spontaneous symmetry breaking (e.g. the Nambu–Jona–Lasinio model) [5], the relativistic Hamilton dynamics [6, 7], the finite-energy [8] and light-cone [9] sum rules and lattice QCD [10]. Here we consider the possibility of investigating light mesons on the basis of the three-dimensional relativistic wave equation with the QCD motivated potential. Our relativistic quark model was originally constructed for the investigation of hadrons with heavy quarks. It was successfully applied for the calculation of their masses and various electroweak decays [11–15]. In these studies the heavy quark expansion has been used to simplify calculations.

[a] e-mail: galkin@physik.hu-berlin.de

[1] Recent calculations of the nonperturbative $q\bar{q}$ potential in continuum Yang–Mills theory in Coulomb gauge can be found in [1].

We determined all parameters of our model from a few experimental observables (some masses and decay rates) and keep them fixed in all our subsequent calculations, thus ensuring its universality. While describing the properties of heavy–light mesons [12], we treated the light quarks in a completely relativistic way. Recently this approach was applied for calculating the masses of light mesons [16] and light diquarks inside the heavy baryons [13]. Due to the phenomenological character of our model we cannot reveal the origin of the chiral symmetry breaking and thus the model cannot describe the chiral limit and the Goldstone nature of the pion. We consider the pion as the purely bound state of the quark and antiquark with fixed constituent masses.

In this paper we extend our previous studies of light mesons and describe their electroweak properties such as the weak decay constants and electromagnetic form factors. The investigation of decay constants and form factors is an important issue since it provides a very sensitive test of the light meson wave functions and, thus, of the quark dynamics in a meson. It requires the completely relativistic consideration of the corresponding decay processes including account for the relativistic transformation of the meson wave functions. The comparison with the available large set of experimental data tests the model predictions in a broad momentum range and helps to discriminate between different model assumptions.

The paper is organized as follows. In Sect. 2 we briefly describe our relativistic quark model, formulate our main assumptions and give the values of parameters. Then in Sect. 3 we present our results for the light meson masses [16], for selfconsistency. There the procedure of constructing the completely relativistic local potential of the light quark interaction in a meson is described. The obtained potential is applied for calculating the light S-wave meson masses and wave functions. In Sect. 4 the novel relativistic expressions for the weak decay constants of pseudoscalar and vector meson are derived. Special attention is paid to including all possible intermediate quark states. It is argued that the negative-energy contributions play an essential role. The calculated decay constants are compared with other predictions and experimental data. The electromagnetic form factors of pseudoscalar mesons are studied in Sect. 5. The relativistic expressions for these form factors are obtained which take into account the contributions of negative-energy quark states and relativistic transformations of the meson wave functions from the rest frame to the moving one. The calculated form factors are plotted in comparison with experimental data. The charged radii of the pion, charged and neutral kaon are also determined. Our conclusions are given in Sect. 6.

2 Relativistic quark model

In the quasipotential approach a meson is described by the wave function of the bound quark–antiquark state, which satisfies the quasipotential equation of the Schrödinger type [11]

$$\left(\frac{b^2(M)}{2\mu_{\rm R}}-\frac{\mathbf{p}^2}{2\mu_{\rm R}}\right)\Psi_M(\mathbf{p})=\int\frac{{\rm d}^3q}{(2\pi)^3}V(\mathbf{p},\mathbf{q};M)\Psi_M(\mathbf{q})\,, \tag{1}$$

where the relativistic reduced mass is

$$\mu_{\rm R}=\frac{E_1E_2}{E_1+E_2}=\frac{M^4-(m_1^2-m_2^2)^2}{4M^3}\,, \tag{2}$$

and E_1, E_2 are given by

$$E_1=\frac{M^2-m_2^2+m_1^2}{2M},\quad E_2=\frac{M^2-m_1^2+m_2^2}{2M}\,. \tag{3}$$

Here $M=E_1+E_2$ is the meson mass, $m_{1,2}$ are the quark masses, and $\mathbf{p}$ is their relative momentum. In the center-of-mass system the relative momentum squared on mass shell reads

$$b^2(M)=\frac{\left[M^2-(m_1+m_2)^2\right]\left[M^2-(m_1-m_2)^2\right]}{4M^2}\,. \tag{4}$$

The kernel $V(\mathbf{p},q;M)$ in (1) is the quasipotential operator of the quark–antiquark interaction. It is constructed with the help of the off-mass-shell scattering amplitude, projected onto the positive-energy states. Constructing the quasipotential of the quark–antiquark interaction, we have assumed that the effective interaction is the sum of the usual one-gluon exchange term with the mixture of long-range vector and scalar linear confining potentials, where the vector confining potential contains the Pauli interaction. The quasipotential is then defined by[2]

$$V(\mathbf{p},\mathbf{q};M)=\bar u_1(p)\bar u_2(-p)\mathcal{V}(\mathbf{p},\mathbf{q};M)u_1(q)u_2(-q)\,, \tag{5}$$

with

$$\mathcal{V}(\mathbf{p},\mathbf{q};M)\equiv$$
$$\mathcal{V}(\mathbf{p}-\mathbf{q})=\frac{4}{3}\alpha_{\rm s}D_{\mu\nu}(\mathbf{k})\gamma_1^\mu\gamma_2^\nu+V_{\rm conf}^V(\mathbf{k})\Gamma_1^\mu\Gamma_{2;\mu}+V_{\rm conf}^S(\mathbf{k})\,,$$

where $\alpha_{\rm s}$ is the QCD coupling constant, $D_{\mu\nu}$ is the gluon propagator in the Coulomb gauge,

$$\begin{aligned}D^{00}(\mathbf{k})&=-\frac{4\pi}{\mathbf{k}^2}\,,\\ D^{ij}(\mathbf{k})&=-\frac{4\pi}{k^2}\left(\delta^{ij}-\frac{k^ik^j}{\mathbf{k}^2}\right)\,,\\ D^{0i}&=D^{i0}=0\,,\end{aligned} \tag{6}$$

and $\mathbf{k}=\mathbf{p}-\mathbf{q}$; γ_μ and $u(p)$ are the Dirac matrices and spinors

$$u^\lambda(p)=\sqrt{\frac{\epsilon(p)+m}{2\epsilon(p)}}\begin{pmatrix}1\\ \dfrac{\boldsymbol{\sigma}\mathbf{p}}{\epsilon(p)+m}\end{pmatrix}\chi^\lambda\,, \tag{7}$$

[2] In our notation, where strong annihilation processes are neglected, antiparticles are described by usual spinors taking into account the proper quark charges.

with $\epsilon(p)=\sqrt{p^2+m^2}$. The effective long-range vector vertex is given by

$$\Gamma_\mu(\mathbf{k})=\gamma_\mu+\frac{\mathrm{i}\kappa}{2m}\sigma_{\mu\nu}k^\nu\,, \tag{8}$$

where κ is the Pauli interaction constant characterizing the anomalous chromomagnetic moment of quarks. Vector and scalar confining potentials in the nonrelativistic limit reduce to

$$\begin{aligned} V^V_{\mathrm{conf}}(r)&=(1-\varepsilon)(Ar+B)\,,\\ V^S_{\mathrm{conf}}(r)&=\varepsilon(Ar+B)\,, \end{aligned} \tag{9}$$

reproducing

$$V_{\mathrm{conf}}(r)=V^S_{\mathrm{conf}}(r)+V^V_{\mathrm{conf}}(r)=Ar+B\,, \tag{10}$$

where ε is the mixing coefficient.

All the model parameters have the same values as in our previous papers [11, 12]. The light constituent quark masses $m_u=m_d=0.33\,\mathrm{GeV}\,, m_s=0.5\,\mathrm{GeV}$ and the parameters of the linear potential $A=0.18\,\mathrm{GeV}^2$ and $B=-0.3\,\mathrm{GeV}$ have the usual values of quark models. The value of the mixing coefficient of vector and scalar confining potentials $\varepsilon=-1$ has been determined from the consideration of charmonium radiative decays [11]. Finally, the universal Pauli interaction constant $\kappa=-1$ has been fixed from the analysis of the fine splitting of heavy quarkonia ${}^3P_J$-states [11]. In the literature the 't Hooft-like interaction between quarks induced by instantons is widely discussed [17]. This interaction can be partly described by introducing the quark anomalous chromomagnetic moment having an approximate value $\kappa=-0.744$ (as found by Diakonov in [17]). This value is of the same sign and order of magnitude as the Pauli constant $\kappa=-1$ in our model. Thus the Pauli term incorporates at least part of the instanton contribution to the $q\bar{q}$ interaction.[3]

3 Light meson masses

The quasipotential (5) can be used for arbitrary quark masses. The substitution of the Dirac spinors (7) into (5) results in an extremely nonlocal potential in the configuration space. Clearly, it is very hard to deal with such potentials without any additional transformations. In oder to simplify the relativistic $q\bar{q}$ potential, we make the following replacement in the Dirac spinors:

$$\epsilon_{1,2}(p)=\sqrt{m^2_{1,2}+\mathbf{p}^2}\to E_{1,2} \tag{11}$$

(see the discussion of this point in [12, 16]). This substitution makes the Fourier transformation of the potential (5) local. We also limit our consideration only to the S-wave states, which further simplifies our analysis, since all terms proportional to $\mathbf{L}^2$ vanish as well as the spin-orbit ones. Thus we neglect the mixing of states with different values of L. Calculating the potential, we keep only operators quadratic in the relative momentum acting on V_{Coul}, $V^{V,S}_{\mathrm{conf}}$ and replace $\mathbf{p}^2\to E^2_{1,2}-m^2_{1,2}$ in higher order operators in accord with (11) preserving the symmetry under the $(1\leftrightarrow 2)$ exchange.

The substitution (11) works well for the confining part of the potential. However, it leads to a fictitious singularity $\delta^3(\mathbf{r})$ at the origin arising from the one-gluon exchange part ($\Delta V_{\mathrm{Coul}}(r)$), which is absent in the initial potential. Note that this singularity is not important if it is treated perturbatively. Since we are not using the expansion in v/c and are solving the quasipotential equation with the complete relativistic potential, an additional analysis is required. Such singular contributions emerge from the following terms:

$$\begin{aligned} &\frac{\mathbf{k}^2}{[\epsilon_i(q)(\epsilon_i(q)+m_i)\epsilon_i(p)(\epsilon_i(p)+m_i)]^{1/2}}V_{\mathrm{Coul}}(\mathbf{k}^2)\,,\\ &\frac{\mathbf{k}^2}{[\epsilon_1(q)\epsilon_1(p)\epsilon_2(q)\epsilon_2(p)]^{1/2}}V_{\mathrm{Coul}}(\mathbf{k}^2)\,, \end{aligned} \tag{12}$$

if we simply apply the replacement (11). However, the Fourier transforms of expressions (12) are less singular at $r\to 0$. To avoid such fictitious singularities we note that if the binding effects are taken into account, it is necessary to replace $\epsilon_{1,2}\to E_{1,2}-\eta_{1,2}V$, where V is the quark interaction potential and $\eta_{1,2}=m_{2,1}/(m_1+m_2)$. At small distances $r\to 0$, the Coulomb singularity in V dominates and makes possible the correct asymptotic behavior. Therefore, we replace $\epsilon_{1,2}\to E_{1,2}-\eta_{1,2}V_{\mathrm{Coul}}$ in the Fourier transforms of terms (12) [18]. We used the similar regularization of singularities in the analysis of heavy–light meson spectra [12]. Finally, we ignore the annihilation terms in the quark potential since they contribute only in the isoscalar channels and are suppressed in the $s\bar{s}$ vector channel [2].

The resulting $q\bar{q}$ potential then reads

$$V(r)=V_{\mathrm{SI}}(r)+V_{\mathrm{SD}}(r)\,, \tag{13}$$

where the spin-independent potential for S-states ($\mathbf{L}^2=0$) has the form

$$\begin{aligned} V_{\mathrm{SI}}(r)=&V_{\mathrm{Coul}}(r)+V_{\mathrm{conf}}(r)+\frac{\left(E_1^2-m_1^2+E_2^2-m_2^2\right)^2}{4(E_1+m_1)(E_2+m_2)}\\ &\times\left\{\frac{1}{E_1E_2}V_{\mathrm{Coul}}(r)\right.\\ &+\frac{1}{m_1m_2}\left(1+(1+\kappa)\left[(1+\kappa)\frac{(E_1+m_1)(E_2+m_2)}{E_1E_2}\right.\right.\\ &\left.\left.-\left(\frac{E_1+m_1}{E_1}+\frac{E_1+m_2}{E_2}\right)\right]\right)V^V_{\mathrm{conf}}(r)\\ &\left.+\frac{1}{m_1m_2}V^S_{\mathrm{conf}}(r)\right\} \end{aligned}$$

[3] As is well known, the instanton-induced 't Hooft interaction term breaks the axial $U_A(1)$-symmetry, the violation of which is needed for describing the η–η' mass splitting. We do not consider this issue here.

$$+\frac{1}{4}\left(\frac{1}{E_1(E_1+m_1)}\Delta\tilde{V}^{(1)}_{\rm Coul}(r)+\frac{1}{E_2(E_2+m_2)}\Delta\tilde{V}^{(2)}_{\rm Coul}(r)\right)-\frac{1}{4}\left[\frac{1}{m_1(E_1+m_1)}+\frac{1}{m_2(E_2+m_2)}-(1+\kappa)\left(\frac{1}{E_1m_1}+\frac{1}{E_2m_2}\right)\right]\Delta V^V_{\rm conf}(r)+\frac{\left(E_1^2-m_1^2+E_2^2-m_2^2\right)}{8m_1m_2(E_1+m_1)(E_2+m_2)}\Delta V^S_{\rm conf}(r)\,, \quad (14)$$

and the spin-dependent potential is given by

$$V_{\rm SD}(r)=\frac{2}{3E_1E_2}\left[\Delta\bar{V}_{\rm Coul}(r)+\left(\frac{E_1-m_1}{2m_1}-(1+\kappa)\frac{E_1+m_1}{2m_1}\right)\times\left(\frac{E_2-m_2}{2m_2}-(1+\kappa)\frac{E_2+m_2}{2m_2}\right)\Delta V^V_{\rm conf}(r)\right]\mathbf{S}_1\mathbf{S}_2\,, \quad (15)$$

with

$$V_{\rm Coul}(r)=-\frac{4}{3}\frac{\alpha_{\rm s}}{r}\,,$$
$$\tilde{V}^{(i)}_{\rm Coul}(r)=V_{\rm Coul}(r)\frac{1}{\left(1+\eta_i\frac{4}{3}\frac{\alpha_{\rm s}}{E_i}\frac{1}{r}\right)\left(1+\eta_i\frac{4}{3}\frac{\alpha_{\rm s}}{E_i+m_i}\frac{1}{r}\right)}\qquad(i=1,2)\,,$$
$$\bar{V}_{\rm Coul}(r)=V_{\rm Coul}(r)\frac{1}{\left(1+\eta_1\frac{4}{3}\frac{\alpha_{\rm s}}{E_1}\frac{1}{r}\right)\left(1+\eta_2\frac{4}{3}\frac{\alpha_{\rm s}}{E_2}\frac{1}{r}\right)}\,,\qquad \eta_{1,2}=\frac{m_{2,1}}{m_1+m_2}\,. \quad (16)$$

Here we put $\alpha_{\rm s}\equiv\alpha_{\rm s}(\mu^2_{12})$ with $\mu_{12}=2m_1m_2/(m_1+m_2)$. We adopt for $\alpha_{\rm s}(\mu^2)$ the simplest model with freezing [19], namely

$$\alpha_{\rm s}(\mu^2)=\frac{4\pi}{\beta_0\ln\frac{\mu^2+M_{\rm B}^2}{\Lambda^2}},\qquad \beta_0=11-\frac{2}{3}n_f, \quad (17)$$

where the background mass is $M_{\rm B}=2.24\sqrt{\Lambda}=0.95\,{\rm GeV}$ [19], and $\Lambda=413\,{\rm MeV}$ was fixed from fitting the ρ mass.[4] We put the number of flavors $n_f=2$ for π, ρ, K, K^* and $n_f=3$ for ϕ. As a result we obtain $\alpha_{\rm s}(\mu^2_{ud})=0.730$, $\alpha_{\rm s}(\mu^2_{us})=0.711$ and $\alpha_{\rm s}(\mu^2_{ss})=0.731$.

The quasipotential equation (1) is solved numerically for the complete relativistic potential (13) which depends on the meson mass in a complicated highly nonlinear way.

[4] The definition (17) of $\alpha_{\rm s}$ can be smoothly matched with the $\alpha_{\rm s}$ used for heavy quarkonia [11] at the scale about m_c.

Table 1. Masses of light S-wave mesons (in MeV)

Meson	State	Theory				Experiment
	$n^{2S+1}L_J$	this work	[2]	[3]	[4]	PDG [20]
π	1^1S_0	154	150	138	140	139.57
ρ	1^3S_1	776†	770	742	785	775.8(5)
π'	2^1S_0	1292	1300		1331	1300(100)
ρ'	2^3S_1	1486	1450		1420	1465(25)
π''	3^1S_0	1788	1880		1826	1812(14)
ρ''	3^3S_1	1921	2000		1472	
K	1^1S_0	482	470	497	506	493.677(16)
K^*	1^3S_1	897	900	936	890	891.66(26)
K'	2^1S_0	1538	1450		1470	
$K^{*\prime}$	2^3S_1	1675	1580		1550	1717(27)
K''	3^1S_0	2065	2020		1965	
$K^{*\prime\prime}$	3^3S_1	2156	2110		1588	
ϕ	1^3S_1	1038	1020	1072	990	1019.46(2)
ϕ'	2^3S_1	1698	1690		1472	1680(20)

† fitted value

The obtained meson masses are presented in Table 1 in comparison with experimental data [20] and other theoretical results [2–4]. This comparison exhibits a reasonably good overall agreement of our predictions with experimental mass values. Our results are also consistent with mass formulas derived using the finite-energy sum rules in QCD [8] and with predictions of lattice QCD [10]. We consider such agreement to be quite successful, since in evaluating the meson masses we had at our disposal only one adjustable parameter Λ, which was fixed from fitting the ρ meson mass. All other parameters are kept the same as in our previous papers [11, 12]. The obtained wave functions of the light mesons are used for the calculation of their decay constants and electromagnetic form factors in the following sections.

4 Decay constants

The decay constants f_P and f_V of the pseudoscalar (P) and vector (V) mesons parameterize the matrix elements of the weak current $J^{\rm W}_\mu=\bar{q}_1\mathcal{J}^{\rm W}_\mu q_2=\bar{q}_1\gamma_\mu(1-\gamma_5)q_2$ between the corresponding meson and the vacuum. They are defined by

$$\langle 0|\bar{q}_1\gamma^\mu\gamma_5 q_2|P(\mathbf{K})\rangle={\rm i}f_PK^\mu\,, \quad (18)$$
$$\langle 0|\bar{q}_1\gamma^\mu q_2|V(\mathbf{K},\varepsilon)\rangle=f_VM_V\varepsilon^\mu\,, \quad (19)$$

where $\mathbf{K}$ is the meson momentum, ε^μ and M_V are the polarization vector and mass of the vector meson. This matrix element can be expressed through the two-particle Bethe–Salpeter wave function in the quark loop integral (see Fig. 1):

$$\langle 0|J^{\rm W}_\mu|M(\mathbf{K})\rangle=\int\frac{{\rm d}^4p}{(2\pi)^4}{\rm Tr}\left\{\gamma_\mu(1-\gamma_5)\Psi(M,p)\right\}, \quad (20)$$

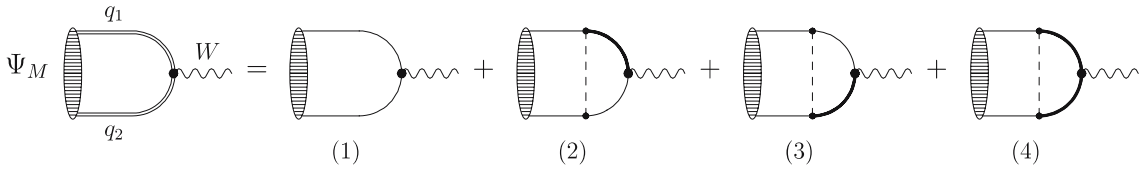

Fig. 1. Weak annihilation diagram of the light meson. *Solid* and *bold lines* denote the positive- and negative-energy part of the quark propagator, respectively. *Dashed lines* represent the interaction operator $\mathcal{V}$

where the trace is taken over spin indices. Integration over p^0 in (20) allows one to pass to the single-time wave function in the meson rest frame:

$$\Psi(M,\mathbf{p}) = \int \frac{\mathrm{d}p^0}{2\pi}\Psi(M,p). \tag{21}$$

This wave function contains both positive- and negative-energy quark states. Since in the quasipotential approach we use the single-time wave function $\Psi_{M\,\mathbf{K}}(\mathbf{p})$ projected onto the positive-energy states it is necessary to include additional terms which account for the contributions of negative-energy intermediate states. The weak annihilation amplitude (20) is schematically presented in the left hand side of Fig. 1. The first diagram on the right hand side corresponds to the simple replacing of the single-time wave function (21) $\Psi(M,\mathbf{p})$ by the quasipotential one $\Psi_{M\,\mathbf{K}}(\mathbf{p})$.[5] The second and third diagrams account for negative-energy contributions to the first and second quark propagators, respectively. The last diagram corresponds to negative-energy contributions from both quark propagators.

Thus in the quasipotential approach this decay amplitude has the form

$$\begin{aligned}
&\langle 0|J^{\mathrm{W}}_{\mu}|M(\mathbf{K})\rangle \\
&\quad = \sqrt{2M}\Bigg\{\int \frac{\mathrm{d}^3p}{(2\pi)^3}\bar{u}_1(p_1)\mathcal{J}^{\mathrm{W}}_{\mu}u_2(p_2)\Psi_{M\,\mathbf{K}}(\mathbf{p}) \\
&\quad + \Bigg[\int \frac{\mathrm{d}^3p\,\mathrm{d}^3p'}{(2\pi)^6}\bar{u}_1(p_1)\Gamma_1\frac{\Lambda^{(-)}_1(p'_1)\gamma^0\mathcal{J}^{\mathrm{W}}_{\mu}\Lambda^{(+)}_2(p'_2)\gamma^0}{M+\epsilon_1(p')-\epsilon_2(p')} \\
&\quad \times \Gamma_2 u_2(p_2)\tilde{V}(p-p')\Psi_{M\,\mathbf{K}}(\mathbf{p}) + (1\leftrightarrow 2)\Bigg] \\
&\quad + \int \frac{\mathrm{d}^3p\,\mathrm{d}^3p'}{(2\pi)^6}\bar{u}_1(p_1)\Gamma_1\frac{\Lambda^{(-)}_1(p'_1)\gamma^0\mathcal{J}^{\mathrm{W}}_{\mu}\Lambda^{(-)}_2(p'_2)\gamma^0}{M+\epsilon_1(p')+\epsilon_2(p')} \\
&\quad \times \Gamma_2 u_2(p_2)\tilde{V}(p-p')\Psi_{M\,\mathbf{K}}(\mathbf{p})\Bigg\},
\end{aligned} \tag{22}$$

where $\mathbf{p}^{(\prime)}_{1,2} = \mathbf{K}/2 \pm \mathbf{p}^{(\prime)}$; matrices $\Gamma_{1,2}$ denote the Dirac structure of the interaction potential (5) for the first and second quark, respectively, and thus $\Gamma_1\Gamma_2\tilde{V}(p-p') = \mathcal{V}(\mathbf{p}-\mathbf{p}')$. The factor $\sqrt{2M}$ follows from the normalization of the quasipotential wave function. The positive- and negative-energy projectors have the standard definition:

$$\Lambda^{(\pm)}(p) = \frac{\epsilon(p) \pm \left(m\gamma^0 + \gamma^0(\boldsymbol{\Delta}\mathbf{p})\right)}{2\epsilon(p)}\,.$$

The quasipotential wave function in the rest frame of the decaying meson $\Psi_M(\mathbf{p}) \equiv \Psi_{M\,\mathbf{0}}(\mathbf{p})$ can be expressed through a product of radial $\Phi_M(p)$, spin $\chi_{ss'}$ and color $\phi_{q_1q_2}$ wave functions

$$\Psi_M(\mathbf{p}) = \Phi_M(p)\chi_{ss'}\phi_{q_1q_2}\,. \tag{23}$$

Now the decay constants can be presented in the following form

$$f_{P,V} = f^{(1)}_{P,V} + f^{(2+3)}_{P,V} + f^{(4)}_{P,V}\,, \tag{24}$$

where the terms on the right hand side originate from the corresponding diagrams in Fig. 1 and parameterize respective terms in (22). In the literature [2, 21–23] usually only the first term is taken into account, since it provides the nonrelativistic limit, while other terms give only relativistic corrections and thus vanish in this limit. Such an approximation can be justified for mesons containing heavy quarks. However, as it will be shown below, for light mesons other terms become equally important, and their account is crucial for getting the results in agreement with experimental data.

The matrix element (22) and thus the decay constants can be calculated in an arbitrary frame and from any component of the weak current. Such calculation can be most easily performed in the rest frame of the decaying meson from the zero component of the current. The same results will be obtained from the vector component, however, this calculation is more cumbersome since here the rest frame cannot be used and, thus, it is important to take into account the relativistic transformation of the meson wave function from the rest frame to the moving one with the momentum $\mathbf{K}$ (see (34) below). It is also possible to perform calculations in the explicitly covariant way using methods proposed in [24].

[5] The contributions with the exchange by the effective interaction potential $\mathcal{V}$ which contain only positive-energy intermediate states are automatically accounted for by the wave function itself.

The resulting expressions for decay constants are given by

$$f_{P,V}^{(1)} = \sqrt{\frac{12}{M}} \int \frac{\mathrm{d}^3p}{(2\pi)^3} \left(\frac{\epsilon_1(p)+m_1}{2\epsilon_1(p)}\right)^{1/2} \left(\frac{\epsilon_2(p)+m_2}{2\epsilon_2(p)}\right)^{1/2} \times \left\{1+\lambda_{P,V}\frac{\mathbf{p}^2}{[\epsilon_1(p)+m_1][\epsilon_2(p)+m_2]}\right\} \Phi_{P,V}(p)\,, \tag{25}$$

$$f_{P,V}^{(2+3)} = \sqrt{\frac{12}{M}} \int \frac{\mathrm{d}^3p}{(2\pi)^3} \left(\frac{\epsilon_1(p)+m_1}{2\epsilon_1(p)}\right)^{1/2} \left(\frac{\epsilon_2(p)+m_2}{2\epsilon_2(p)}\right)^{1/2} \times \left[\frac{M-\epsilon_1(p)-\epsilon_2(p)}{M+\epsilon_1(p)-\epsilon_2(p)} \times \frac{\mathbf{p}^2}{\epsilon_1(p)[\epsilon_1(p)+m_1]} \times \left\{1+\lambda_{P,V}\frac{\epsilon_1(p)+m_1}{\epsilon_2(p)+m_2}\right\} + (1 \leftrightarrow 2)\right] \Phi_{P,V}(p)\,, \tag{26}$$

$$f_{P,V}^{(4)} = \sqrt{\frac{12}{M}} \int \frac{\mathrm{d}^3p}{(2\pi)^3} \left(\frac{\epsilon_1(p)+m_1}{2\epsilon_1(p)}\right)^{1/2} \left(\frac{\epsilon_2(p)+m_2}{2\epsilon_2(p)}\right)^{1/2} \times \frac{M-\epsilon_1(p)-\epsilon_2(p)}{M+\epsilon_1(p)+\epsilon_2(p)} \times \left\{-\lambda_{P,V}-\frac{\mathbf{p}^2}{[\epsilon_1(p)+m_1][\epsilon_2(p)+m_2]}\right\} \times \left[\frac{(1-\varepsilon)m_1^2m_2^2}{\epsilon_1^2(p)\epsilon_2^2(p)}+\frac{\mathbf{p}^2}{[\epsilon_1(p)+m_1][\epsilon_2(p)+m_2]}\right] \times \Phi_{P,V}(p)\,, \tag{27}$$

with $\lambda_P=-1$ and $\lambda_V=1/3$. Here ε is the mixing coefficient of scalar and vector confining potentials (9) and the long-range anomalous chromomagnetic quark moment κ (8) is put equal to -1. Note that $f_P^{(2+3)}$ vanishes for pseudoscalar mesons with equal quark masses, such as the pion. The positive-energy contribution (25) reproduces the previously known expressions for the decay constants [2, 21]. The negative-energy contributions (26) and (27) are new and play a significant role for light mesons (see below).

In the nonrelativistic limit $p^2/m^2 \to 0$ the expression (25) for decay constants gives the well-known formula

$$f_{P,V}^{\mathrm{NR}} = \sqrt{\frac{12}{M_{P,V}}}\,|\Psi_{P,V}(0)|\,, \tag{28}$$

where $\Psi_{P,V}(0)$ is the meson wave function at the origin $r=0$. All other contributions vanish in the nonrelativistic limit.

In Table 2 we present our predictions for the light meson decay constants calculated using the meson wave functions which were obtained as the numerical solutions of the quasipotential equation in Sect. 3. The nonrelativistic values f_M^{NR}, (28), as well as the values of different contributions in Fig. 1, $f_M^{(1,2,3,4)}$, see (25)–(27), and the full relativistic results f_M, (24), are given. In Table 3 we compare our results for the decay constants f_M with predictions of other approaches [2–4, 7, 25], recent values from two- [10] and three-flavor lattice QCD [26] and available experimental data [20]. It is clearly seen that the nonrelativistic predictions are significantly overestimating all decay constants, especially for the pion (almost by a factor of 10). The account of the part of relativistic corrections by keeping in (24) only the first term $f_M^{(1)}$ (25), which is usually used for semirelativistic calculations, does not dramatically improve the situation. The disagreement is still large. This is connected with the anomalously small masses of light pseudoscalar mesons exhibiting their chiral nature. In the semirelativistic quark model [2, 21] the pseudoscalar meson mass is replaced by the so-called mock mass $\tilde{M}_P$, which is equal to the mean total energy of free quarks in a meson, and with our wave functions: $\tilde{M}_\pi = 2\langle\epsilon_q(p)\rangle \approx 1070\,\mathrm{MeV}$ ($\sim 8M_\pi$) and $\tilde{M}_K = \langle\epsilon_q(p)\rangle + \langle\epsilon_s(p)\rangle \approx 1232\,\mathrm{MeV}$ ($\sim 2.5M_K$). Such a replacement gives $f_P^{(1)}$ values which are still ≈ 1.4 times larger than the experimental ones [2]. As we see from Table 2, in the quasipotential approach it is not justified to neglect contributions of the negative-energy intermediate states for light meson decay constants. Indeed, the values of $f_M^{(2+3)}+f_M^{(4)}$ are large and negative (reaching -76% of $f_\pi^{(1)}$ for the pion) thus compensating the overestimation of decay constants by the positive-energy contribution $f_M^{(1)}$. This is the consequence of the smallness of the light pseudoscalar meson masses compared to the energies of their constituents. The negative-energy contributions (26) and (27) are proportional to the ratio of the meson binding energy $M-\epsilon_1(p)-\epsilon_2(p)$ to its mass. For mesons with heavy quarks this factor leads to the suppression of negative-energy contributions since the binding energies are small on the heavy meson mass scale. This results in the dominance of the positive-energy term $f_M^{(1)}$ since the negative-energy terms give only $1/m_Q$ contributions (m_Q is the heavy quark mass).[6] On the other hand, for light mesons, especially for the pion and kaon, the binding energies are large on the light meson mass scale and, thus, such factor gives no suppression. Taking the complete relativistic expression for decay constants f_M (24) brings theoretical predictions in good agreement with available experimental data.

Table 2. Different contributions to the pseudoscalar and vector decay constants of light mesons (in MeV). The notations are taken according to (24) and (28)

Constant	f_M^{NR}	$f_M^{(1)}$	$f_M^{(2+3)}+f_M^{(4)}$	$(f_M^{(2+3)}+f_M^{(4)})/f_M^{(1)}$	f_M
f_π	1290	515	−391	−76%	124
f_K	783	353	−198	−56%	155
f_ρ	490	402	−183	−46%	219
f_{K^*}	508	410	−174	−42%	236
f_ϕ	511	415	−170	−41%	245

The comparison of our values of the decay constants with other predictions in Table 3 indicate that they are

[6] For the heavy–heavy B_c meson ($c\bar{b}$) these negative-energy corrections will be of order v^4/c^4 and thus very small. The influence of the negative-energy contributions $f_M^{(2+3,4)}$ on the decay constants of heavy–light B and D mesons will be considered elsewhere.

Table 3. Pseudoscalar and vector decay constants of light mesons (in MeV)

Constant	This work	[2]	[3, 25]	[4]	[7]	Lattice [10]	Lattice [26]	Experiment [20]
f_π	124	180	131	219	138	126.6 ± 6.4	129.5 ± 3.6	$130.7 \pm 0.1 \pm 0.36$
f_K	155	232	155	238	160	152.0 ± 6.1	156.6 ± 3.7	$159.8 \pm 1.4 \pm 0.44$
f_ρ	219	220	207		238	239.4 ± 7.3		$220 \pm 2^*$
f_{K^*}	236	267	241		241	255.5 ± 6.5		$230 \pm 8^\dagger$
f_ϕ	245	336	259			270.8 ± 6.5		$229 \pm 3^\ddagger$

* derived from the experimental value for $\Gamma_{\rho^0 \to e^+e^-}$,
† derived from the experimental value for the ratio $\Gamma_{\tau \to K^* \nu_\tau}/\Gamma_{\tau \to \rho \nu_\tau}$ and the f_ρ value,
‡ derived from the experimental value for $\Gamma_{\phi \to e^+e^-}$

competitive even with the results of more sophisticated approaches [4, 25] which are based on the Dyson–Schwinger and Bethe–Salpeter equations. On the other hand our model is more selfconsistent than some other approaches [2, 6, 7, 21, 22]. We calculate the meson wave functions by solving the quasipotential equation in contrast to the models based on the relativistic Hamilton dynamics [6, 7] where various ad hoc wave function parameterizations are employed. We also do not need to introduce the mock meson mass [2, 21, 22] and to substitute it for the light meson mass as it was discussed above.

5 Electromagnetic form factors

The elastic matrix element of the electromagnetic current J_μ between the initial and final pseudoscalar meson states is parameterized by the form factor $F_P(Q^2)$

$$\langle M(P_\mathrm{F})|J_\mu|M(P_\mathrm{I})\rangle = F_P(Q^2)(P_\mathrm{I}+P_\mathrm{F})_\mu\,, \qquad (29)$$

where $Q^2 = -(P_\mathrm{F}-P_\mathrm{I})^2$.

In the quasipotential approach such a matrix element has the form [27]

$$\langle M(P_\mathrm{F})|J_\mu|M(P_\mathrm{I})\rangle = \int \frac{\mathrm{d}^3p\,\mathrm{d}^3q}{(2\pi)^6}\bar{\Psi}_{M\,\mathbf{P}_\mathrm{F}}(\mathbf{p})\Gamma_\mu(\mathbf{p},\mathbf{q})\Psi_{M\,\mathbf{P}_\mathrm{I}}(\mathbf{q})\,, \qquad (30)$$

where $\Gamma_\mu(\mathbf{p},\mathbf{q})$ is the two-particle vertex function and Ψ_M are the meson wave functions projected onto the positive-energy states of quarks and boosted to the moving reference frame. The contributions to Γ come from Figs. 2 and 3. The term $\Gamma^{(2)}$ includes contributions from the negative-energy quark states. Note that the form of the relativistic corrections resulting from the vertex function $\Gamma^{(2)}$ explicitly depends on the Lorentz structure of the $q\bar{q}$-interaction. Thus the vertex function is given by

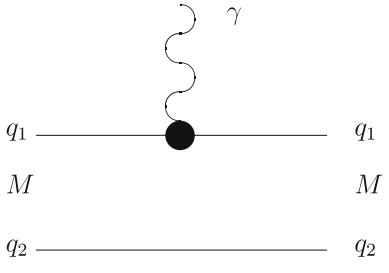

Fig. 2. Lowest order vertex function $\Gamma^{(1)}$ corresponding to (32). Photon interaction with one quark is shown

$$\Gamma_\mu(\mathbf{p},\mathbf{q}) = \Gamma^{(1)}_\mu(\mathbf{p},\mathbf{q}) + \Gamma^{(2)}_\mu(\mathbf{p},\mathbf{q}) + \cdots\,, \qquad (31)$$

where

$$\Gamma^{(1)}_\mu(\mathbf{p},\mathbf{q}) = e_1\bar{u}_1(p_1)\gamma_\mu u_1(q_1)(2\pi)^3\delta(\mathbf{p}_2-\mathbf{q}_2) + (1 \leftrightarrow 2)\,, \qquad (32)$$

and

$$\Gamma^{(2)}_\mu(\mathbf{p},\mathbf{q}) = e_1\bar{u}_1(p_1)\bar{u}_2(p_2) \times \left\{\mathcal{V}(\mathbf{p}_2-\mathbf{q}_2)\frac{\Lambda^{(-)}_1(k'_1)}{\epsilon_1(k'_1)+\epsilon_1(q_1)}\gamma^0_1\gamma_{1\mu} + \gamma_{1\mu}\frac{\Lambda^{(-)}_1(k_1)}{\epsilon_1(k_1)+\epsilon_1(p_1)}\gamma^0_1\mathcal{V}(\mathbf{p}_2-\mathbf{q}_2)\right\} \times u_1(q_1)u_2(q_2) + (1 \leftrightarrow 2)\,. \qquad (33)$$

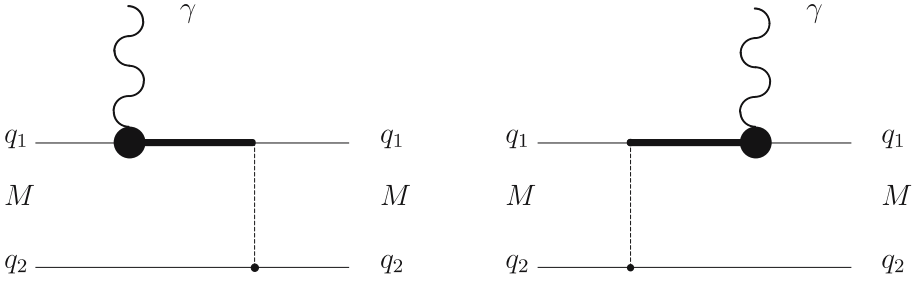

Fig. 3. Vertex function $\Gamma^{(2)}$ corresponding to (33). *Dashed lines* represent the interaction operator $\mathcal{V}$. *Bold lines* denote the negative-energy part of the quark propagator. As on Fig. 1, photon interaction with one quark is shown

Here $e_{1,2}$ are the quark charges, $\mathbf{k}_1 = \mathbf{p}_1 - \mathbf{\Delta}; \mathbf{k}'_1 = \mathbf{q}_1 + \mathbf{\Delta}$; $\mathbf{\Delta} = \mathbf{P}_\mathrm{F} - \mathbf{P}_\mathrm{I}$;

$$\Lambda^{(-)}(p) = \frac{\epsilon(p) - \left(m\gamma^0 + \gamma^0(\mathbf{\Delta}\mathbf{p})\right)}{2\epsilon(p)}, \quad \epsilon(p) = \sqrt{p^2+m^2},$$

and

$$p_{1,2} = \epsilon_{1,2}(p)\frac{P_\mathrm{F}}{M} \pm \sum_{i=1}^{3} n^{(i)}(P_\mathrm{F})p^i,$$

$$q_{1,2} = \epsilon_{1,2}(q)\frac{P_\mathrm{I}}{M} \pm \sum_{i=1}^{3} n^{(i)}(P_\mathrm{I})q^i,$$

where $n^{(i)}$ are three four-vectors given by

$$n^{(i)\mu}(p) = \left\{\frac{p^i}{M},\ \delta_{ij} + \frac{p^i p^j}{M(E+M)}\right\},$$

$$E = \sqrt{\mathbf{p}^2 + M^2}, \qquad i,j = 1,2,3;$$

$P_\mathrm{I} = (E_\mathrm{I}, \mathbf{P}_\mathrm{I})$ and $P_\mathrm{F} = (E_\mathrm{F}, \mathbf{P}_\mathrm{F})$ are four-momenta of the initial and final mesons.

It is important to note that the wave functions entering the current matrix element (30) cannot be both in the rest frame. In the initial meson rest frame, the final meson is moving with the recoil momentum $\mathbf{\Delta}$. The wave function of the moving meson $\Psi_{M\,\mathbf{\Delta}}$ is connected with the wave function in the rest frame $\Psi_{M\,\mathbf{0}} \equiv \Psi_M$ by the transformation [27]

$$\Psi_{M\,\mathbf{\Delta}}(\mathbf{p}) = D_1^{1/2}(R^\mathrm{W}_{L_\mathbf{\Delta}}) D_2^{1/2}(R^\mathrm{W}_{L_\mathbf{\Delta}}) \Psi_{M\,\mathbf{0}}(\mathbf{p}), \qquad (34)$$

where R^W is the Wigner rotation, $L_\mathbf{\Delta}$ is the Lorentz boost from the rest frame to a moving one, and the rotation matrix $D^{1/2}(R)$ in the spinor representation is given by

$$\begin{pmatrix} 1 & 0 \\ 0 & 1 \end{pmatrix} D^{1/2}_{1,2}(R^\mathrm{W}_{L_\mathbf{\Delta}}) = S^{-1}(\mathbf{p}_{1,2}) S(\mathbf{\Delta}) S(\mathbf{p}), \qquad (35)$$

where

$$S(\mathbf{p}) = \sqrt{\frac{\epsilon(p)+m}{2m}} \left(1 + \frac{\boldsymbol{\alpha}\mathbf{p}}{\epsilon(p)+m}\right)$$

is the usual Lorentz transformation matrix of the Dirac spinor.

To calculate the matrix element (29) of the electromagnetic current between the pseudoscalar meson states we substitute the vertex functions $\Gamma^{(1)}$ (32) and $\Gamma^{(2)}$ (33) in (30) and take into account the wave function transformation (34). Then we use the δ function in $\Gamma^{(1)}$ to perform one of the integrations in the matrix element (30). For the contribution of $\Gamma^{(2)}$ we use instead the quasipotential equation to replace the integral of the product of the interaction potential and the bound state wave function by the product of the corresponding binding energy and the wave function. To simplify the calculation we explicitly use the value $\kappa = -1$ for the long-range anomalous chromomagnetic quark moment (8). However, as previously we keep the dependence on the mixing parameter ε of the vector and scalar confining potentials (9). As a result we get the following expression for the electromagnetic form factor of the pseudoscalar meson:

$$F_P(Q^2) = F_P^{(1)}(Q^2) + \varepsilon F_P^{(2)S}(Q^2) + (1-\varepsilon) F_P^{(2)V}(Q^2), \qquad (36)$$

$$F_P^{(1)}(Q^2) = \frac{2\sqrt{EM}}{E+M}\Bigg\{e_1 \int \frac{\mathrm{d}^3p}{(2\pi)^3} \bar{\Psi}_M\left(\mathbf{p} + \frac{2\epsilon_2(p)}{E+M}\mathbf{\Delta}\right) \times \sqrt{\frac{\epsilon_1(p)+m_1}{\epsilon_1(p+\Delta)+m_1}} \Bigg[\frac{\epsilon_1(p+\Delta)+\epsilon_1(p)}{2\sqrt{\epsilon_1(p+\Delta)\epsilon_1(p)}} + \frac{\mathbf{p}\mathbf{\Delta}}{2\sqrt{\epsilon_1(p+\Delta)\epsilon_1(p)}(\epsilon_1(p)+m_1)} - \frac{\epsilon_1(p+\Delta)-\epsilon_1(p)}{2\sqrt{\epsilon_1(p+\Delta)\epsilon_1(p)}} \frac{\mathbf{p}_\mathrm{T}^2}{\epsilon_1(p)+m_1} \times \left(\frac{1}{\epsilon_1(p)+m_1} + \frac{1}{\epsilon_2(p)+m_2}\right)\Bigg] \Psi_M(\mathbf{p}) + (1 \leftrightarrow 2)\Bigg\}, \qquad (37)$$

$$F_P^{(2)S}(Q^2) = \frac{2\sqrt{EM}}{E+M}\Bigg\{e_1 \int \frac{\mathrm{d}^3p}{(2\pi)^3} \bar{\Psi}_M\left(\mathbf{p} + \frac{2\epsilon_2(p)}{E+M}\mathbf{\Delta}\right) \times \sqrt{\frac{\epsilon_1(p)+m_1}{\epsilon_1(p+\Delta)+m_1}} \frac{\epsilon_1(p+\Delta)+m_1}{2\epsilon_1(p+\Delta)} \times \Bigg[\frac{\epsilon_1(p+\Delta)-\epsilon_1(p)+2m_1}{2\sqrt{\epsilon_1(p+\Delta)\epsilon_1(p)}} - \frac{\mathbf{p}\mathbf{\Delta}}{2\sqrt{\epsilon_1(p+\Delta)\epsilon_1(p)}(\epsilon_1(p)+m_1)} - \frac{\epsilon_1(p+\Delta)+m_1}{2\sqrt{\epsilon_1(p+\Delta)\epsilon_1(p)}} \frac{\mathbf{p}_\mathrm{T}^2}{\epsilon_1(p)+m_1} \times \left(\frac{1}{\epsilon_1(p)+m_1} + \frac{1}{\epsilon_2(p)+m_2}\right)\Bigg] \times \frac{\epsilon_1(p+\Delta)-\epsilon_1(p)}{\epsilon_1(p+\Delta)\left[\epsilon_1(p+\Delta)+\epsilon_1(p)\right]} \times \left[M - \epsilon_1(p) - \epsilon_2(p)\right] \Psi_M(\mathbf{p}) + (1 \leftrightarrow 2)\Bigg\}, \qquad (38)$$

$$F_P^{(2)V}(Q^2) = \frac{2\sqrt{EM}}{E+M}\Bigg\{e_1 \int \frac{\mathrm{d}^3p}{(2\pi)^3} \bar{\Psi}_M\left(\mathbf{p} + \frac{2\epsilon_2(p)}{E+M}\mathbf{\Delta}\right) \times \sqrt{\frac{\epsilon_1(p)+m_1}{\epsilon_1(p+\Delta)+m_1}} \frac{\epsilon_1(p+\Delta)+m_1}{2\epsilon_1(p+\Delta)} \times \Bigg[\frac{\epsilon_1(p)-m_1}{2\sqrt{\epsilon_1(p+\Delta)\epsilon_1(p)}} + \frac{\mathbf{p}\mathbf{\Delta}}{2\sqrt{\epsilon_1(p+\Delta)\epsilon_1(p)}(\epsilon_1(p)+m_1)} + \frac{\epsilon_1(p+\Delta)+m_1}{2\sqrt{\epsilon_1(p+\Delta)\epsilon_1(p)}} \frac{\mathbf{p}_\mathrm{T}^2}{\epsilon_1(p)+m_1}$$

$$\times\left(\frac{1}{\epsilon_1(p)+m_1}+\frac{1}{\epsilon_2(p)+m_2}\right)\Bigg]$$
$$\times\frac{\epsilon_1(p+\Delta)-\epsilon_1(p)}{\epsilon_1(p+\Delta)[\epsilon_1(p+\Delta)+\epsilon_1(p)]}$$
$$\times[M-\epsilon_1(p)-\epsilon_2(p)]\Psi_M(\mathbf{p})+(1\leftrightarrow 2)\Bigg\}, \quad (39)$$

where $F_P^{(2)S(V)}$ are contributions from scalar (vector) confining potentials and $\mathbf{p}_{\rm T}=\mathbf{p}^2-(\mathbf{p}\boldsymbol{\Delta})^2/\boldsymbol{\Delta}^2$, $E=\sqrt{M^2+\boldsymbol{\Delta}^2}$. As previously, we put $\varepsilon=-1$ for further numerical calculations. It is important to note that the above expressions for the electromagnetic form factor of the positively-charged pseudoscalar meson exactly satisfy the normalization condition

$$F_P(0)=1 \quad (40)$$

following from the electric charge conservation.

Now we can use the wave functions of the pseudoscalar light mesons (π, K), found in Sect. 3, for the numerical calculation of their electromagnetic form factors $F_P(Q^2)$ in the space-like region $Q^2\geq 0$. The results of such calculations for the charged pion are shown in Figs. 4 ($F_\pi^2(Q^2)$) and 5 ($Q^2F_\pi(Q^2)$) in comparison with experimental data from [28–30]. Good agreement with data both in low and high Q^2 regions is found, including recent JLab data [30], which are plotted with crosses. It is clearly seen from Fig. 5 that the calculated pion form factor at high Q^2 exhibits the asymptotic behavior $F_\pi(Q^2)\sim\alpha_{\rm s}(Q^2)/Q^2$ predicted by the quark counting rule [31] and perturbative QCD [32]. Our results for the pion form factor can also be compared with QCD based calculations [33] and with recent parameterizations [34, 35] which arise from the constraints of analyticity and unitarity. The latter form factor models are based on the vector meson dominance and include a pattern of radial excitations expected from dual resonance models [35]. The consistency of our results with such parameterizations (cf. Fig. 4 with Fig. 2 of [35]) just means the manifestation of the quark–hadron duality. Finally, our

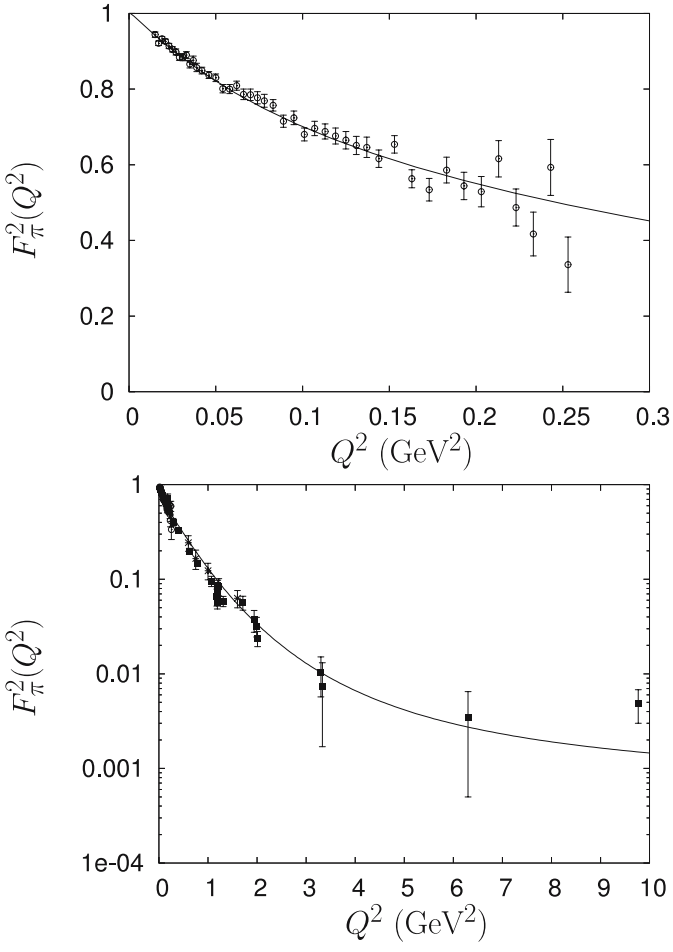

Fig. 4. The charged pion form factor squared in comparison with experimental data from [28] (*open circles*), [29] (*solid squares*) and [30] (*crosses*)

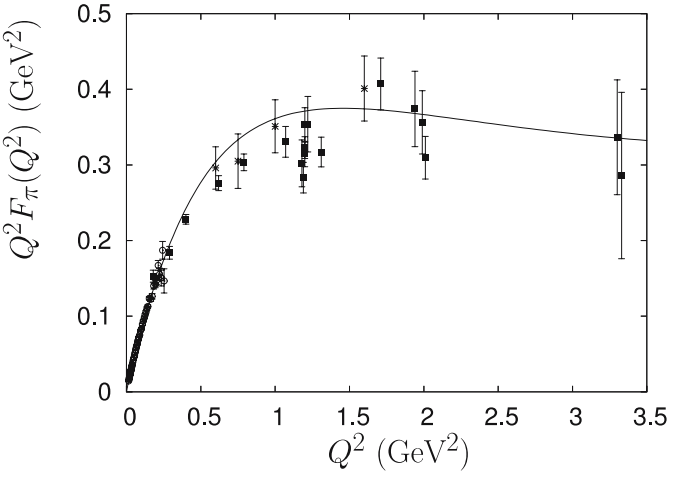

Fig. 5. Q^2 times charged pion form factor in comparison with experimental data from [28] (*open circles*), [29] (*solid squares*) and [30] (*crosses*)

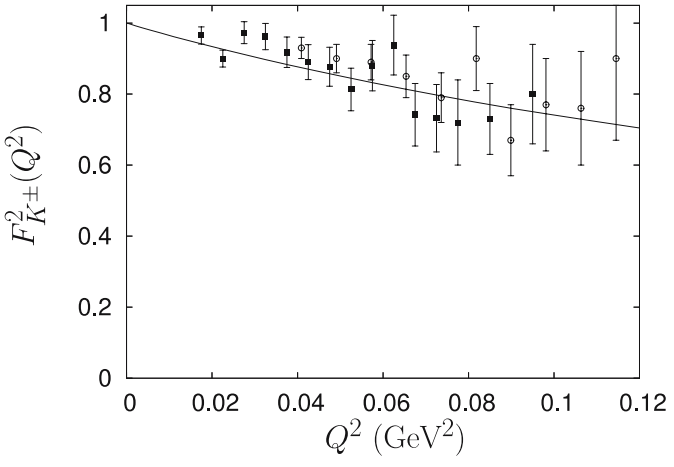

Fig. 6. The charged kaon form factor squared in comparison with experimental data from [38] (*open circles*) and [39] (*solid squares*)

Table 4. Charge radii of light pseudoscalar mesons

Charge radii	This work	[2]	[25]	[7]	Lattice [37]	Experiment [20]
$\sqrt{\langle r^2\rangle_\pi}$ (fm)	0.66	0.66	0.67	0.63	0.63 ± 0.1	0.672 ± 0.08
$\sqrt{\langle r^2\rangle_{K^\pm}}$ (fm)	0.57	0.59	0.62	0.60		0.560 ± 0.031
$\langle r^2\rangle_{K^0}$ (fm^2)	-0.072	-0.09	-0.086	-0.062		-0.076 ± 0.018

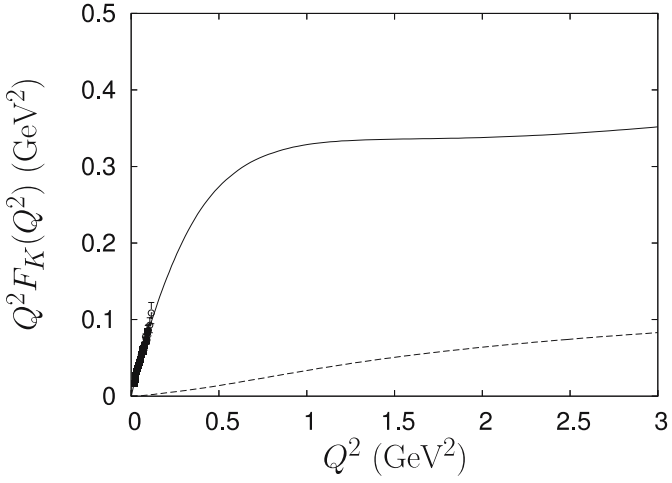

Fig. 7. Q^2 times the charged kaon (*solid line*) and neutral kaon (*dashed line*) form factors

predictions agree fairly well with recent lattice computations of the pion form factor [36, 37]. The corresponding plots for the charged kaon form factor are given in Figs. 6 and 7 in comparison with experimental data from [38, 39], which are available only for the low Q^2 region. Again good agreement with experimental data is found. On Fig. 7 we also plot the neutral kaon form factor by the dashed line.

The mean-squared charge radius of the pseudoscalar meson ($P = \pi, K$) is defined by

$$\langle r^2\rangle_P = -6\left[\frac{\mathrm{d}F_P(Q^2)}{\mathrm{d}Q^2}\right]_{Q^2=0}. \qquad (41)$$

The calculated values of the charge radii of light pseudoscalar mesons are given in Table 4 in comparison with predictions of other approaches [2, 7, 25, 37] and experimental data [20]. An overall good agreement with experimental data is found.

6 Conclusions

The relativistic quark model, which has been previously developed and successfully used for the comprehensive investigation of different properties of heavy and heavy–light hadrons, was applied here for calculating the masses, weak decay constants and electromagnetic form factors of the light mesons. The main assumptions and parameters of the model (such as the Lorentz structure and parameters of the confining potential and quark masses) were kept the same as in previous studies. The only change we made is the necessary modification of the running coupling constant $\alpha_s(\mu^2)$ in the infrared region. Following [19] we chose the simplest model with freezing (17). Therefore only one additional parameter Λ was introduced and it was fixed from fitting the ρ meson mass. We constructed the local relativistic quasipotential for the light quarks using the replacement (11), which was previously tested on the heavy–light mesons. The resulting relativistic potential (13) depends on the meson mass in a complicated nonlinear way. Solving numerically the quasipotential equation (1) we got masses of the ground-state and radially-excited light mesons in a reasonably good overall agreement with experimental data. Even the masses of the pseudoscalar π and K mesons are well reproduced. This is a nontrivial result, since we use the constituent quark masses in our description and thus the chiral symmetry is explicitly broken from the very beginning. We determined the light meson wave functions and used them for studying their electroweak properties.

First the weak decay constants of pseudoscalar and vector mesons were investigated. It was argued that both positive- and negative-energy parts of the quark propagators in the weak annihilation loop should be taken into account. Usually in the semirelativistic quark model [2, 21, 22] only the positive-energy contributions are kept. This approximation requires to replace in the expression for the pseudoscalar decay constant (25) the meson mass by the so-called mock meson mass, which is considerably larger, in order not to get the significant overestimate of the decay constants. We showed that the negative-energy contributions to the light meson pseudoscalar decay constants are large and negative. Their account brings theoretical predictions (with the physical meson masses) in good agreement with available experimental data.

Next we studied the electromagnetic form factor of the pseudoscalar mesons. The corresponding matrix element of the electromagnetic current was calculated using the quasipotential approach. The additional contributions of the intermediate negative-energy states (33) were taken into account as well as the transformation of the meson wave function from the rest frame to a moving one (34). As a result the relativistic expression for the electromagnetic form factor was obtained. We then calculated the pion, charged and neutral kaon form factors in the space-like region. Good agreement with available experimental data both in small and large Q^2 regions were found. At large momentum transfer this form factor tends to reproduce the power-law behavior predicted by perturtbative QCD [32]. The calculated charge radii of light pseudoscalar mesons are in good agreement with experiment.

In conclusion, we found that the obtained results are quite competitive with the predictions of other approaches [2–4, 6, 7, 10, 25, 26, 36, 37] including more sophisticated ones, which were specially developed for treating light mesons.

Acknowledgements. The authors are grateful to A. Ali Khan, A. Badalian, M. Müller-Preussker, V. Savrin and Y. Simonov for useful discussions. Two of us (R.N.F. and V.O.G.) were supported in part by the Deutsche Forschungsgemeinschaft under contract Eb 139/2-3 and by the Russian Foundation for Basic Research under Grant No. 05-02-16243.

References

1. C. Feuchter, H. Reinhardt, Phys. Rev. D **70**, 105 021 (2004)
2. S. Godfrey, N. Isgur, Phys. Rev. D **32**, 189 (1985)
3. P. Maris, C.D. Roberts, Int. J. Mod. Phys. E **12**, 297 (2003); P. Maris, P.C. Tandy, Phys. Rev. C **60**, 055 214 (1999)
4. M. Koll et al., Eur. Phys. J. A **9**, 73 (2000)
5. D. Ebert, H. Reinhardt, Nucl. Phys. B **271**, 188 (1986); D. Ebert, H. Reinhardt, M.K. Volkov, Prog. Part. Nucl. Phys. **33**, 1 (1994); M.K. Volkov, D. Ebert, M. Nagy, Int. J. Mod. Phys. A **13**, 5443 (1998); M.K. Volkov, C. Weiss, Phys. Rev. D **56**, 221 (1997)
6. A.F. Krutov, V.E. Troitsky, Phys. Rev. C **65**, 045 501 (2002)
7. J. He, B. Julia-Diaz, Y. Dong, Eur. Phys. J. A **24**, 411 (2005)
8. N.V. Krasnikov, A.A. Pivovarov, Phys. Lett. B **112**, 397 (1982); N.V. Krasnikov, A.A. Pivovarov, N.N. Tavkhelidze, Z. Phys. C **19**, 301 (1983); A.L. Kataev, hep-ph/9805218
9. V.M. Braun, A. Khodjamirian, M. Maul, Phys. Rev. D **61**, 073 004 (2000)
10. A. Ali Khan et al., Phys. Rev. D **65**, 054 505 (2002); **67**, 059 901 (2003); for a recent review see A. Ali Khan, hep-lat/0507031 and references therein
11. D. Ebert, R.N. Faustov, V.O. Galkin, Phys. Rev. D **67**, 014 027 (2003)
12. D. Ebert, V.O. Galkin, R.N. Faustov, Phys. Rev. D **57**, 5663 (1998); **59**, 019 902 (1999)
13. D. Ebert, R.N. Faustov, V.O. Galkin, Phys. Rev. D **72**, 034 026 (2005)
14. R.N. Faustov, V.O. Galkin, A.Y. Mishurov, Phys. Rev. D **53**, 6302 (1996)
15. D. Ebert, R.N. Faustov, V.O. Galkin, A.P. Martynenko, Phys. Rev. D **66**, 014 008 (2002); Phys. Atom. Nucl. **68**, 784 (2005)
16. D. Ebert, R.N. Faustov, V.O. Galkin, Mod. Phys. Lett. A **20**, 1887 (2005)
17. D. Diakonov, Progr. Part. Nucl. Phys. **51**, 173 (2003); N.I. Kochelev, Phys. Lett. B **426**, 149 (1998)
18. H.A. Bethe, E.E. Salpeter, Quantum Mechanics of One- and Two-Electron Atoms (Springer-Verlag, Berlin, 1957)
19. A.M. Badalian, A.I. Veselov, B.L.G. Bakker, Phys. Rev. D **70**, 016 007 (2004); Y.A. Simonov, Phys. Atom. Nucl. **58**, 107 (1995)
20. Particle Data Group, S. Eidelman et al., Phys. Lett. B **592**, 1 (2004)
21. S. Godfrey, Phys. Rev. D **33**, 1391 (1986)
22. S. Veseli, I. Dunietz, Phys. Rev. D **54**, 6803 (1996)
23. D. Ebert, R.N. Faustov, V.O. Galkin, Mod. Phys. Lett. A **17**, 803 (2002)
24. D. Ebert, R.N. Faustov, V.O. Galkin, A.P. Martynenko, Phys. Rev. D **70**, 014 018 (2004)
25. P. Maris, P. Tandy, Phys. Rev. C **62**, 055 204 (2000)
26. MILC Collaboration, C. Aubin et al., Phys. Rev. D **70**, 114 501 (2004); C.T.H. Davies et al., Phys. Rev. Lett. **92**, **022001** (2004)
27. R.N. Faustov, Ann. Phys. (N.Y.) **78**, 176 (1973); Nuovo Cimento A **69**, 37 (1970)
28. S.R. Amendolia et al., Nucl. Phys. B **277**, 168 (1986)
29. C.J. Bebek et al., Phys. Rev. D **17**, 1693 (1978)
30. J. Volmer et al., Phys. Rev. Lett. **86**, 1713 (2001)
31. V.A. Matveev, R.M. Muradian, A.N. Tavkhelidze, Lett. Nuovo Cim. **7**, 719 (1973); S.J. Brodsky, G.R. Farrar, Phys. Rev. Lett. **31**, 1153 (1973)
32. G.P. Lepage, S.J. Brodsky, Phys. Lett. B **87**, 359 (1979); G.R. Farrar, D.R. Jackson, Phys. Rev. Lett. **43**, 246 (1979); A.V. Efremov, A.V. Radyushkin, Phys. Lett. B **94**, 245 (1980)
33. A.P. Bakulev, K. Passek-Kumericki, W. Schroers, N.G. Stefanis, Phys. Rev. D **70**, 033 014 (2004); N.G. Stefanis, W. Schroers, H.C. Kim, Phys. Lett. B **449**, 299 (1999)
34. A. Pich, J. Portoles, Phys. Rev. D **63**, 093 005 (2001)
35. C. Bruch, A. Khadjamirian, J.H. Kühn, Eur. Phys. J. C **39**, 41 (2005)
36. F.D.R. Bonnet et al., Phys. Rev. D **72**, 054 506 (2005)
37. S. Hashimoto et al., hep-lat/0510085
38. E.B. Dally et al., Phys. Rev. Lett. **45**, 232 (1980)
39. S.R. Amendolia et al., Phys. Lett. B **178**, 435 (1986)